

## Effect of Non-Condensables on Natural Circulation Passive Safety Systems: Modelling and Experimentation in the AP-600 Reactor

L.E. Herranz<sup>a</sup>, J.L. Muñoz-Cobo<sup>b</sup>, J.C. de la Rosa<sup>b</sup>, S. Chiva<sup>b</sup>, A. Escrivá<sup>b</sup>

<sup>a</sup>CIEMAT, Spain

<sup>b</sup>Universidad Politécnica de Valencia, Spain.

**Abstract.** AP600 passive containment cooling system relies heavily on the internal and external natural convection. A good deal of investigations have addressed the system performance and its modelling. This paper shows the major results of one of the most thorough programs carried out and compares its results with predictions obtained by a diffusion based model developed ad-hoc to account for the specific aspects of AP600 containment cooling system.

### 1. INTRODUCTION

In the middle to late eighties new reactor designs relying on passive engineering features to accomplish safety functions were proposed (Taylor,1986). Most of the novel designs incorporated passive containment cooling systems (PCCS) to remove heat from the containment. These systems were essentially based on the steam condensation under different conditions and geometries. The diversity of the PCCS is illustrated by the General Electric's SBWR (Simplified Boiling Water Reactor) (Sawyer,1992), where forced flow in-tube condensation takes place, and by the Westinghouse's AP600 (Advanced Pressurized Reactor) (Kennedy et al.,1994), where condensation on externally cooled metallic surfaces occurs under free convection. Even though steam condensation had been thoroughly studied prior to these designs, the new scenarios involved particular characteristics that required further research, and also reinforced the need of a reliable and accurate simulation of heat transfer under steam condensation conditions with noncondensables.

Several experimental programs have been carried out to address specific advanced reactor scenarios and consistent data have been gathered (Ogg,1991; Vierow et al.,1991; Siddique et al.,1993; Kuhn et al.,1995). This paper is mainly focused on systems where steam condenses on cooled flat surfaces, so that particular attention will be given to the containment cooling system of AP600 (or AP1000). There are several experimental programs specific to this design (WCAP, 1992; Dehbi et al., 1991; Anderson et al., 1998).

Mechanistic condensation modeling has been traditionally addressed by two different approaches: solution of conservation equations in the boundary layer (Sparrow,1964; Ghiaassiaan,1995; Yuahn,1995) and the application of the heat-mass transfer analogy (Kim,1990; Peterson,1992; Herranz,1997). Herr et al. (1993) summarized the fundamentals and the major contributions in each of these two categories. The boundary layer solutions, although insightful from a theoretical point of view, are not useful for containment analysis due to their complexity and expense; conversely, the analogy based models can be easily implemented into the nodal system codes used in containment accident analysis and they provide an insight of phenomenon with a non-time consuming feature. Despite extensive validation of analogy based models (Corradini,1984;Bunker et al.,1986) in the past, the new hypothetical accident scenarios associated with advanced reactors require an upgrade of their formulation and a validation under the anticipated accidents conditions.

The analogy models have made use of correlations of mass transfer obtained by the Chilton-Colburn analogy (Collier et al.,1994) and assume closure laws concerning heat transfer across the film. Fundamentals of this modeling approach are given by Kim et al. (1990) who derived expressions for forced and natural convection condensation in the presence of a noncondensable gas and analyzed the potential impact of film waviness. More recently Peterson et al. (1992) used the Clapeyron equation to develop a more compact expression of condensation heat transfer, in which the condensation driving force, based on concentration differences, is formulated as a function of temperature differences (much more convenient in heat transfer problems).

This paper summarizes the work carried out regarding modelling and experimentation on the passive containment cooling system of the AP600 (or AP1000). First, the cooling system and one of the most relevant experimental programs executed will be described. Particular emphasis will be given to the observations related to the effect of noncondensable gases. Then, the generic equations outlining a heat-mass transfer analogy model will be given along with a discussion on the capability of this approach to deal with the anticipated scenarios. Some examples of the model performance will be also included.

## **2. THE PASSIVE CONTAINMENT COOLING SYSTEM**

The use of natural forces as driving mechanisms of safety systems enhances reliability and, as a consequence, improves safety of nuclear power plants. Passive Containment Cooling (PCC) during accidents is a good example of this approach. One of the reactor concepts that has been designed which implements PCCS and is under study is the Westinghouse's AP600 pressurized water reactor.

This design utilizes a unique system to maintain the containment atmosphere pressure and temperature within design limits (Spencer et al.,1993). Figure 1 shows a schematic of the reactor containment. In the event of a postulated accident where high pressure cooling water escapes into the containment, the pressure and temperature will increase as water flashes to steam. The steam will in turn start to condense on the steel containment vessel which is initially at ambient temperature. This results in an increase in the surface temperature of the steel wall. The heating of the steel containment wall causes air from outside, due to buoyancy forces, to be drawn in through an air baffle between the concrete containment and the steel inner wall (not present in current reactors). This process along with the release of cooling water, by gravity from reservoirs situated above the containment, hold the wall temperature well below that of the internal bulk atmosphere. This temperature difference along with a concentration difference created by the condensation of steam in the presence of noncondensable gases, sets up a natural circulation flow pattern within containment. Steam condensation, enhanced by the turbulent natural convection, but inhibited by a noncondensable gas layer formed adjacent to the wall, should provide sufficient cooling to keep the ambient conditions within containment under safe structural limits.

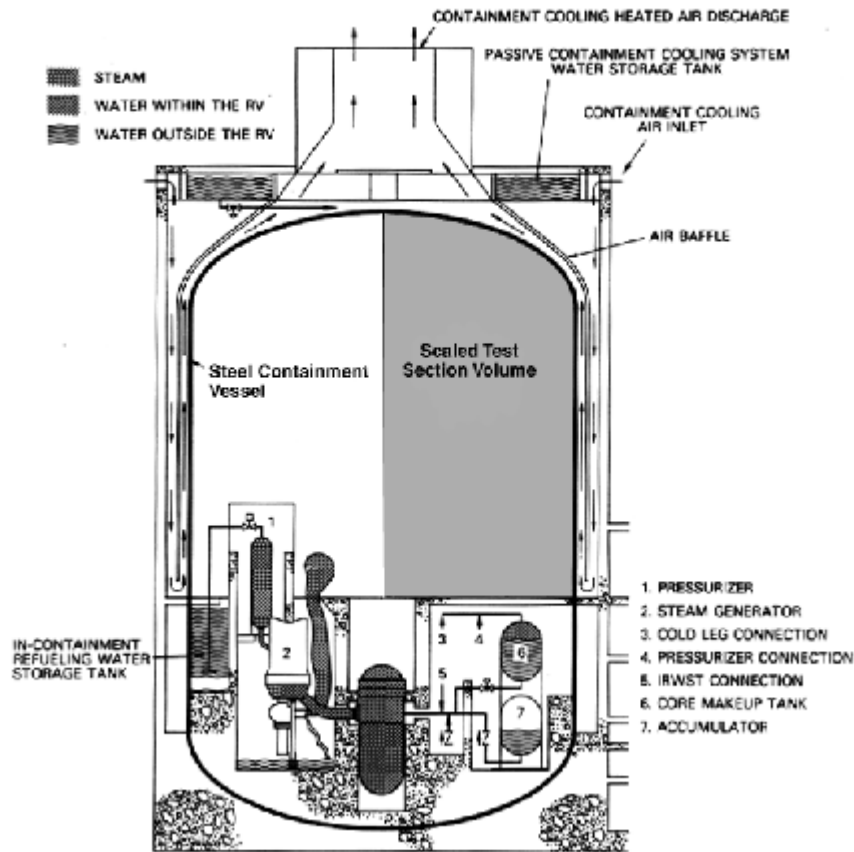


Figure 1. Sketch of the PCCS of the AP600

### 3. UW EXPERIMENTAL PROGRAM

The UW-Madison (Anderson et al., 1998) carried out a relevant experimental program demonstrating the AP600 capability to passively condense the steam and reduce the pressure within the containment.

The AP600 PCCS needed to be tested by conducting experiments which measured the heat transfer rate from the containment bulk to the external atmosphere. Even though there has been extensive experimental and theoretical research in the area of condensation (Collier, 1994), much less work specifically addressed the condensation process at large scales, such as reactor containments. Uchida et al. (1965) and Tagami et al. (1965) provided some of the pioneering work in this area, which has recently been corroborated by other investigators (Kataoka et al., 1995). This work has led to the development of correlations used in containment safety analysis (Corradini, 1984; Kataoka et al., 1995) that estimate the Heat Transfer Coefficient HTC based on the ratio of  $W_{nc}/W_v$ . Green et al. (1996) carried out a peer review and analysis of both small and large scale experiments including CVTR (Carolina Virginia Tube Reactor) and the E-series of the HDR experiments, along with others. They concluded that the above mentioned correlations provide a too simplistic method of estimating the Heat Transfer Coefficient (HTC), missing variables such as pressure, temperature, and bulk velocity which are of primary importance in condensing scenarios.

With the advent of new PCCS cooling designs there has been a change in the potential condensing conditions within containment. The results of which, significantly increases the temperature difference between the wall and the containment compared to those in the current reactors that have no external cooling. Also the absolute temperature of the containment surfaces will be lower, affecting properties relevant in the condensation process. These issues along with other differences in anticipated accident conditions, along with the increased importance on the condensation process of the PCCS, prompted renewed interest in performing experiments

aimed at confirming the PCCS capability to accomplish its goal and to fully characterize the condensation scenario outlined by the revised boundary conditions in these systems.

Westinghouse (Kennedy et al., 1994) performed some large scale experiments designed to look at the entire cooling system to evaluate its performance and provide test data for license approval by the NRC. These large scale tests give general information on the pressure, temperature and containment responses in the case of a postulated accident as a function of time, along with some information on the heat transfer rates, but lack some of the insight given by more closely controlled facilities on the effects of both primary and lower order variables. Some past experiments have been designed to look specifically at these effects at smaller scale. Debhi et al. (1991) conducted some experimental work on a 3.5m long 0.038m diameter tubular geometry with different pressures, mass fractions of vapor/noncondensables, and light noncondensable gases (helium as a hydrogen simulant). This led to the development of correlations that relied on these variables. Despite the valuable information provided by this data the geometry of the facility is a drawback due to the questionable non-uniform conditions in the vessel. Huhtiniemi et al. (1992), considered the effects of orientation and bulk velocity in a smaller rectangular facility. He improved on the cooling design of Debhi, however, the small size required him to impose a forced velocity flow parallel to the cold wall so that he could achieve velocities similar to those anticipated in an actual containment accident.

To bridge the gap between the large time varying simulation of an accident (Westinghouse) and the smaller separate effects studies (Debhi and Huhtiniemi), an experimental program which addressed conditions similar to those expected during an accident in the AP600, at an in-depth level was conducted. Specifically this experimental program was aimed at achieving a thorough understanding of the role of both major and minor variables on the heat transfer rate, along with providing a valuable data base to validate heat transfer models. A thorough description of the facilities (Figure 2) and the experimental techniques used was given by Anderson et al. (1998). A synthesis of the results is given in the next subsections.

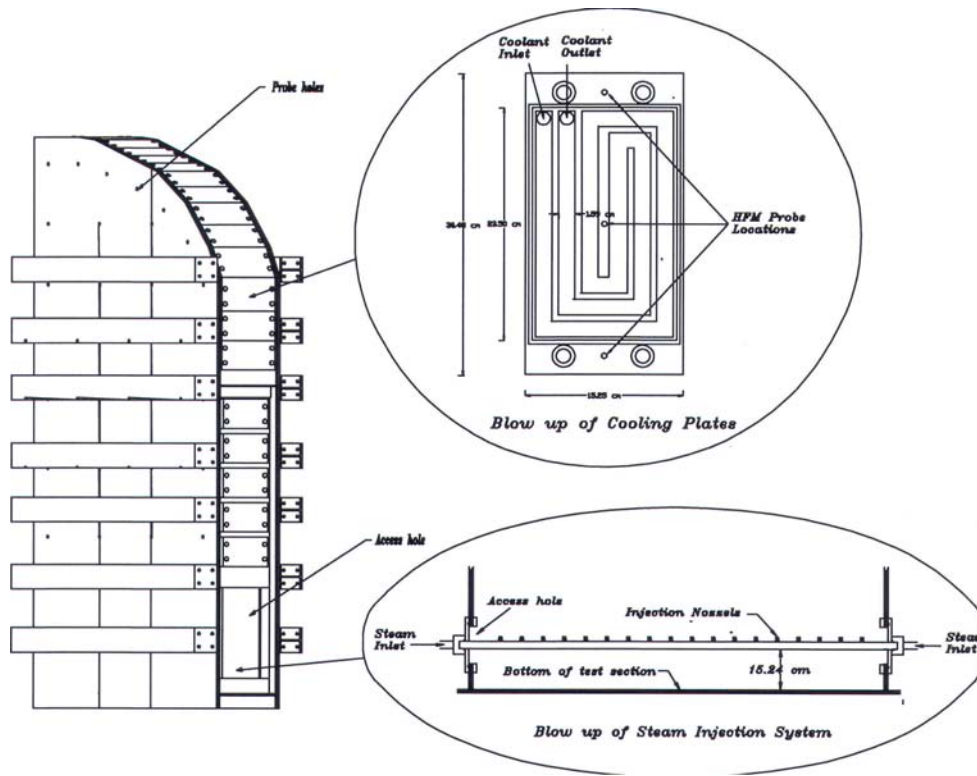


Figure 2. Experimental facility and HTC measurement techniques.

### 3.1. Effects of surface orientation

Little variation between the HTC measured at horizontal and vertical locations was found. Given the dramatically different behavior of the condensate depending upon the surface orientation, the slight 20% variation found was attributed to the fact the presence of noncondensables decreased the importance of the film structure. That is, the relatively high resistance of the noncondensable boundary layer dominates heat transfer. The slight increase observed (20% higher HTC in the horizontal orientation) was thought to be a consequence of the disruption of this gaseous boundary layer due to the departure of the droplets from the horizontal plate. Such an effect would increase the turbulence within the boundary layer and reduce the local thickness, decreasing the gas resistance to heat transfer.

### 3.2. Effects of bulk temperature variations

Figure 3 shows the effects of changing the bulk temperature from 60 – 90°C within the test section (at atmospheric pressure) while maintaining an approximately constant wall temperature of 30°C. As the bulk temperature rises, the heat transfer coefficient also increases. Such an increase is a direct consequence of the amount of steam in the vessel ( $W_{\text{air}}/W_{\text{v}}$ ) (the bulk temperature rise was achieved by injecting hot steam in the vessel until getting the saturation conditions at the desired temperature). Then, as the wall temperature is kept constant, the driving force of the condensation, which is dependent upon the steam concentration difference between gas bulk and wall, is subsequently increased, resulting in more steam condensing onto the wall. In addition, the density difference between the bulk and the wall ( $\rho_{\text{gi}} - \rho_{\text{gb}}$ ) becomes larger, since an increase in the amount of steam causes a smaller bulk gas density. This results in an enhancement of the natural convection motion of the gas along with the increase in the concentration gradient.

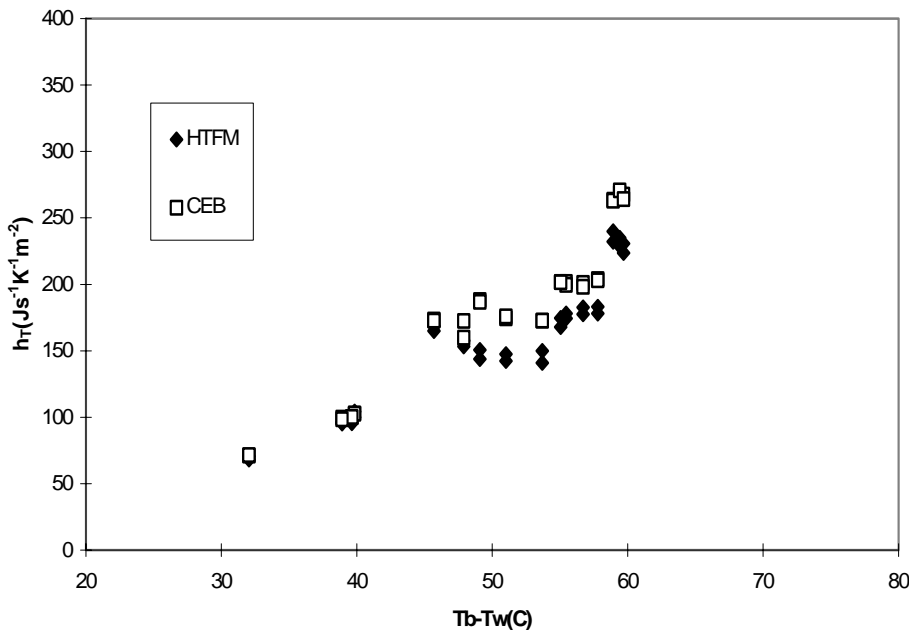


Figure 3. Evolution of HTCs with bulk temperature and steam mass fraction changes.

### 3.3. Effects of bulk temperature variations

Figure 4 shows the variation of the HTC with wall temperatures for both atmospheric and pressurized experiments. The atmospheric tests were conducted with a constant bulk temperature of 90°C and wall temperatures that varied from 30 to 80°C. While the pressurized tests were conducted at a pressure of 3 bars with one atmosphere of noncondensables (air) and a bulk temperature of 115.7°C with various wall temperatures. This figure shows that the HTC decreases with increasing temperature difference between the bulk and the wall (approximately 25% with a change in  $\Delta T$  from 10 to 60°C), although the heat flux increases the increase in the subcooling  $\Delta T$  is larger than the increase in the heat flux thus resulting in lower HTC measurement. The trend is the same at both pressures although the curve for the higher pressures is elevated due to the enhancement to HTC with pressure.

As the wall temperature is increased the concentration of steam at the wall will increase while remaining constant in the bulk. This will reduce the condensation driving force due to the concentration gradient ( $X_{vb}-X_{vi}$ ). Along with a reduction in the concentration gradient there will be a reduction in the natural gas motion which is a function of the density difference between the bulk and the interface ( $\rho_{gi}-\rho_{gb}$ ). This is due to a decrease in the density at the interface as a result of the increased temperature (ideal gas law). Since the density at the interface is closer to the bulk density there is a decrease in the convection driving force. Therefore as the wall temperature increases the heat flux decrease substantially. The HTC which is directly proportional to the heat flux but inversely proportional to the temperature difference ( $T_b - T_i$ ) increases slightly with an increase in wall temperature because the reduction in the heat flux is overwhelmed by the large decrease in the  $\Delta T$ .

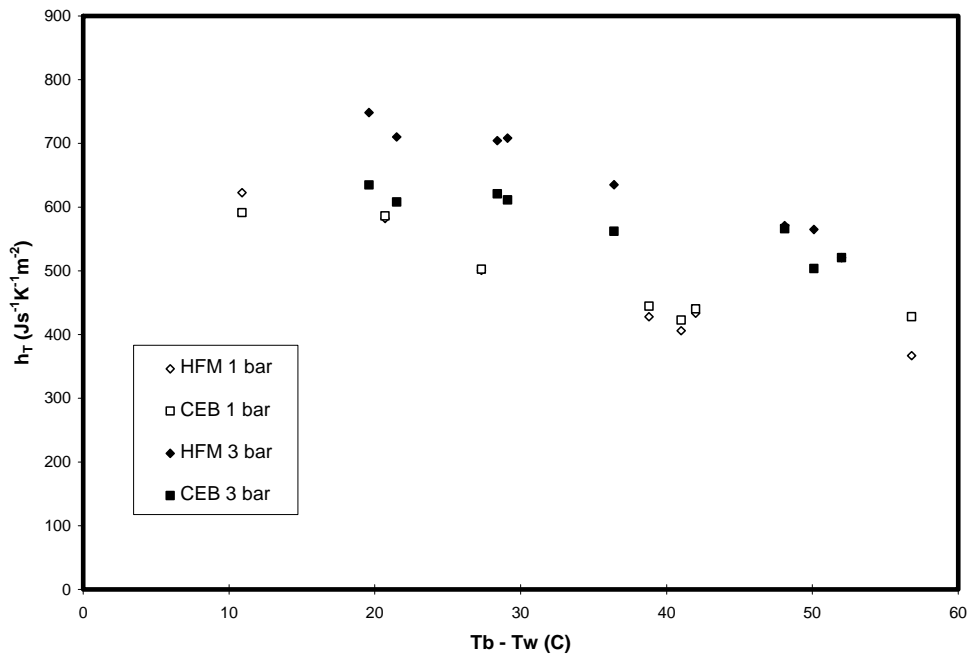


Figure 4. Evolution of HTCs vs. wall temperatures (P=1 bar and P=3 bar)

### 3.4. Effects of pressure

As observed in Figure 5, the HTC increases with pressure, showing a quasi-linear trend for pressure higher than 1.5 bar. This increase can be attributed to the rise in steam concentration that accompanies the increase in the system pressure. Namely, the condensation flux is enhanced by the enlargement of the gradient of steam concentration due to the fact that the steam content in the gas bulk is higher at higher pressures. This

reinforcement of the steam concentration gradient is only partially compensated by the reduction that higher pressures cause on the diffusion coefficient (inversely proportional to pressure). With these effects one should add that the pressure rise involves indirectly a minimization of noncondensable contribution into the gas molar fraction.

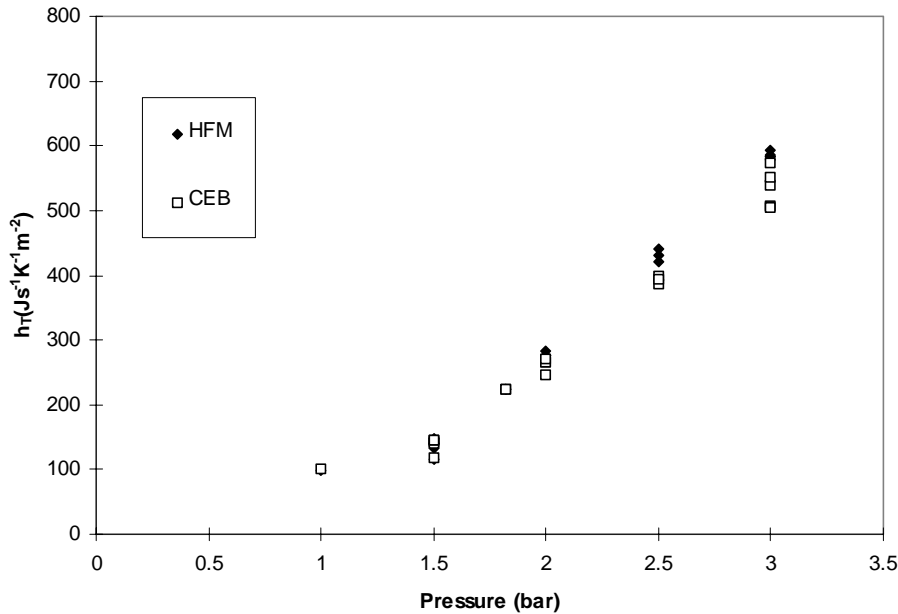


Figure 4. Evolution of HTCs vs. pressure

### 3.5. Effects of helium in the noncondensable mixture

Experiments were conducted with helium gas mixed with air in molar concentrations of the total noncondensable ranging from 0-50%, which corresponds to total helium concentration between 0-30%. In the atmospheric experiments the helium was added to the air prior to the injection of steam. Therefore if 30% of the noncondensable was originally helium this would stay constant for the various bulk temperatures, however the total helium molar fraction would decrease with an increase in the bulk temperature. Several experiments were done with concentration ranging from 0-30% molar of helium in the noncondensable and no noticeable effect was observed. Figure 5 shows the HTC as a function of  $T_b - T_w$  for a constant wall temperature of 30°C and various bulk temperatures for helium concentrations in this range. As can be seen, there are no significant effects on the HTC caused by the introduction of helium. These findings are consistent with those observed by Pernstienner (1994) and were thoroughly explained by Herranz et al. (1998) based on the compensating effects that helium has on the buoyancy driving force and on the diffusion coefficient of steam for helium concentrations up to 40% of the noncondensables.

Experiments were also conducted with helium at more prototypical pressures with the same range of helium in the noncondensable mixture. These tests were performed by first attaining a steady state condition at 3 bars and a saturation temperature of 115.7 °C. Table 1 shows the results and key parameters of the experiments for pressures of 3 bar and concentrations below 40% molar of the noncondensable.

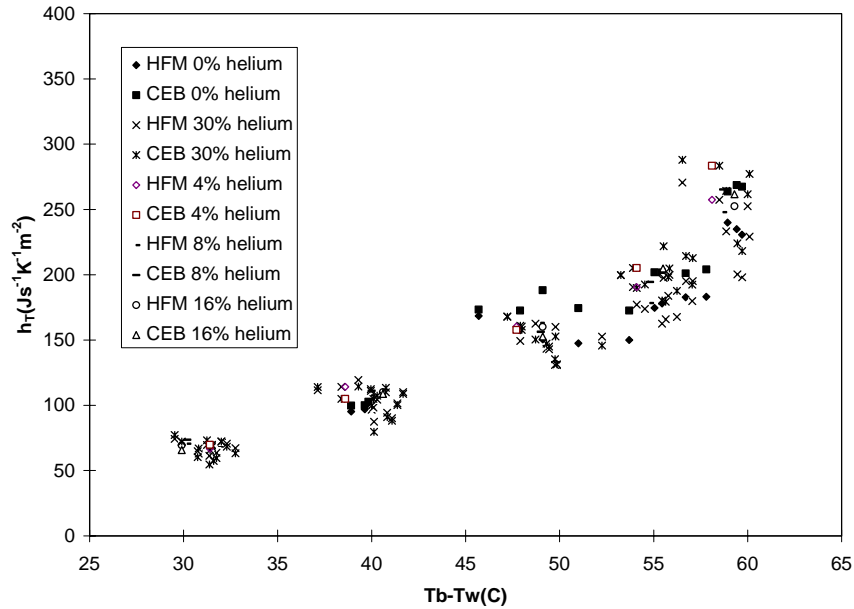


Figure 5. Evolution of HTCs vs. pressure

| <i>TEST</i>  | <i>T<sub>bulk</sub></i> | <i>T<sub>wall</sub></i> | <i>P<sub>He</sub></i> | <i>P<sub>air</sub></i> | <i>P<sub>v</sub></i> | <i>P<sub>tot</sub></i> | HFM    | CEB    |
|--------------|-------------------------|-------------------------|-----------------------|------------------------|----------------------|------------------------|--------|--------|
| <i>T5000</i> | 117.69                  | 77.07                   | 0.00                  | 1.16                   | 1.84                 | 3.0                    | 593.67 | 574.09 |
| <i>T5001</i> | 114.57                  | 71.13                   | 0.13                  | 1.20                   | 1.67                 | 3.0                    | 503.51 | 493.07 |
| <i>T5002</i> | 104.63                  | 59.89                   | 0.27                  | 1.54                   | 1.19                 | 3.0                    | 315.81 | 323.05 |
| <i>T5003</i> | 105.75                  | 61.30                   | 0.40                  | 1.36                   | 1.24                 | 3.0                    | 335.83 | 302.33 |
| <i>T5004</i> | 91.89                   | 45.87                   | 0.83                  | 1.41                   | 0.75                 | 3.0                    | 187.62 | 183.58 |

Table 1: Helium in the noncondensable mixture at 3 bar

A couple of experiments were conducted with concentrations greater than 40% and it was found that as the noncondensable density approaches that of the steam there can exist stratification where a noncondensable gas layer is stable above a steam rich layer. Figure 6 shows the bulk temperature profiles along with the heat transfer coefficients for the individual plates for a test with 57% molar helium and 43% molar air in the noncondensable and with 100% air as the noncondensable. Both tests were performed at the same conditions (e.g. steam flow rate, coolant flow rate) except for the replacement of the air with a mixture of air and helium. The temperature profile clearly shows the stratification of a noncondensable rich layer of gas above a steam rich region. This effect is also observed in the HTC measurements. Plate 1-8 which are in the upper portion of the test section show a dramatically lower HTC then plates 9-14 which are lower in elevation and are adjacent to the steam rich layer. This effect was seen at lower helium concentrations down to about 45% helium in the noncondensable mixture however the pocket of noncondensable rich layer is reduced in size slightly with lower helium concentrations. It is also slightly less stable. This is due to the fact that as the helium concentration reaches this level it is approximately the same density as the steam but as steam is continually added the

temperature of the steam rich region can increase and become lighter than the noncondensable and then there could exist a break down in the stratification and the convection would result in a mixing of the bulk atmosphere.

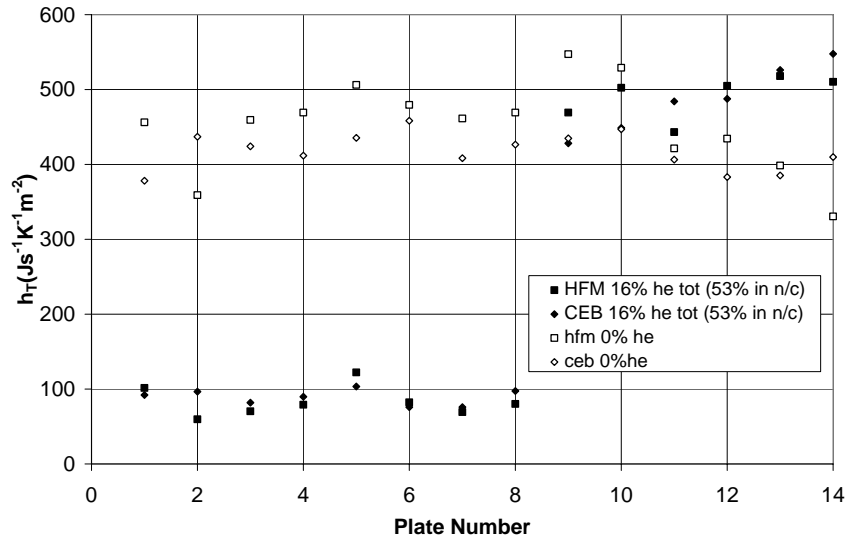


Figure 6. Influence of He stratification in HTC

In summary, the addition of light noncondensable gases has little effect on the HTC up to concentrations of approximately 40% molar added to the air. At this point the density of the noncondensable is approximately the same as the steam and buoyancy forces ( $\rho_{gi} - \rho_{gb}$ ) will tend to zero. At higher helium concentrations when the noncondensable mixture is lighter than the steam there can exist a stable pocket of noncondensables above the steam rich bulk which prohibits condensation and can result in as much as a 50% reduction in the heat transfer. Therefore, the concentrations needed to effect the HTC and form stratification are above that which can exist in the bulk of the containment since they will be above the detonation limit. However, there are sub-compartments where these concentrations might exist. If one wishes to model condensation in these areas the amount of helium and level of stratification could be important.

#### 4. FUNDAMENTALS OF A HEAT-MASS TRANSFER ANALOGY MODEL

A thorough description of a model based on the diffusion theory and the heat-mass transfer analogy was reported by Herranz et al. (1998). Next an overall picture of its basics is given.

##### 4.1. Overall approach

Newton's law of cooling stipulates that the overall heat flux from the gas to the coolant may be expressed by,

$$q_T = h_T (T_g - T_c) \quad (1)$$

where  $h_T$  is the total heat transfer coefficient that, in terms of thermal resistances, is defined as:

$$h_T = \frac{1}{A} \left( \frac{1}{R_c + R_w + R_{foul} + R_g} \right) \quad (2)$$

Namely, the total thermal resistance is estimated as a combination in series of the individual contributions of gas ( $R_g$ ), fouling layer ( $R_{foul}$ ), wall ( $R_w$ ) and coolant ( $R_c$ ). The gas thermal resistance,  $R_g$ , consists of two parallel components, related to the actual heat transfer mechanisms: convection and condensation. This diagram encompasses the whole picture of heat transfer, fouling due to particle deposition included. However, most of experiments conducted so far for passive systems imposed constant wall temperatures and did not use particle-laden gas mixtures.

#### 4.2. Condensate film

The film heat transfer coefficient is calculated by a modified Nusselt equation (Collier et al., 1994),

$$h_{film} = \left[ \frac{\rho_\ell \cdot (\rho_\ell - \rho_{gb}) \cdot g \cdot \sin \theta \cdot h'_{fg} \cdot k_\ell^3}{4 \cdot \mu_\ell \cdot z \cdot (T_i - T_w)} \right]^{1/4} \cdot \Psi \quad (3)$$

where  $h'_{fg}$  accounts for the condensate subcooling and the temperature jump across the film,

$$h'_{fg} = h_{fg} \cdot \left[ 1 + 0.68 \frac{C_{p\ell} \cdot (T_i - T_w)}{h_{fg}} \right] \quad (4)$$

and  $\Psi$  takes into account the enhancement in heat transfer caused by the rippled structure of the film, waviness effect, described by Kutateladze et al. (1979) as:

$$\Psi = Re_\ell^{0.04} \quad (5)$$

#### 4.3. Bulk gas mixture

The parallel combination of convection and condensation thermal resistances may be expressed in terms of the gas heat transfer coefficient,  $h_g$ , as,

$$h_g = h_{conv} + h_{cond} \quad (6)$$

Equivalently, the non-dimensional version of eq. (6) becomes,

$$h_g = Nu_o \frac{k}{L} + Sh_o \frac{k_{cond}}{L} \quad (7)$$

where  $L$  is the characteristic length of the system,  $k$  is the gas conductivity and  $k_{cond}$  is a condensation conductivity. The latter is derived from the diffusion theory of gases in boundary layers and the use of the Clapeyron equation (Peterson et al., 1993).

At this stage of model development, the use of the heat-mass transfer analogy yields a general expression of the form:

$$q_g = \frac{Sh}{L} k_{eff} (T_g - T_i) \quad (8)$$

Here,  $Sh$  is the Sherwood number once the heat-mass transfer analogy has been corrected for high mass fluxes scenarios,  $T_i$  is the interface temperature, and  $k_{eff}$  is an effective conductivity. In general,  $k_{eff}$  may be written as:

$$k_{\text{eff}} = k F\left(\frac{\text{Pr}}{\text{Sc}}\right) + k_{\text{cond}} \quad (9)$$

where  $F\left(\frac{\text{Pr}}{\text{Sc}}\right)$  is a function of the ratio between the Prandtl and Schmidt numbers. Herranz et al. (1998) modified the theoretical approach due to Peterson et al. (1993) and proposed an approximation for  $k_{\text{cond}}$  where the importance of noncondensable gases in the scenarios is explicitly stated as follows:

$$k_{\text{cond}} = \frac{C_g M_s h_{fg}^2 D}{R_s T_i T_g} \frac{\ln\left(\frac{1 - X_{sg}}{1 - X_{si}}\right)}{\ln(X_{sg}/X_{si})} \quad (10)$$

In this expression, the subscripts i and g refer to the interface and the gas bulk conditions, respectively. Further, steam properties are identified by the subscript s, X are the molar fractions, C is the total gas concentration,  $M_s$  is the molecular weight of steam,  $h_{fg}$  is the vaporisation latent heat, D is the diffusion coefficient and R is the universal constant for ideal gases.

Directing the attention to the Sherwood number (Sh) in eq. (17), it can be written as a function of its counterpart in eq. (16) by defining a correction factor,  $\Theta$ , that accounts for disruption of the heat-mass transfer analogy under the anticipated conditions in postulated severe accidents in new containment designs. In equation form, this statement becomes:

$$\text{Sh} = \text{Sh}_o \Theta \quad (11)$$

where  $\Theta$  is often referred to as a suction factor. Its physical interpretation may be explained as follows: as steam condenses its absorption into the liquid film causes a thinning of the boundary layer that, as said above, makes gradients steeper and enhances the transfer processes. Despite that both temperature and concentration profiles are affected by this phenomenon, the effect on concentration is substantially larger than the effects on temperature or velocity.

Two investigators (Aggarwal et al. (1973) and Yeroshenko et al. (1984)) have determined experimentally the relevant influence of suction on heat transfer. The two data sets have been and their results have been correlated by Herranz et al. (1997). However, it is obvious that in order to model steam condensation as mechanistically as possible, analytical expressions are more amenable. In this regard, Bird et al. (1960) have proposed a rather simple equation that emerged from the solution of the system mass, momentum and heat conservation equations. That is

$$\Theta = \frac{X_{nc}^i}{X_{nc}^{\text{avg}}} \quad (12)$$

As expected,  $\Theta$  is a non-dimensional factor that measures the relative decrease in steam content at the interface with respect to that characterizing the bulk of the boundary layer. In contrast, other authors such as Mickley (1954) and Herranz (1996) have suggested an alternative expression for the quantification of  $\Theta$ , namely

$$\Theta = \frac{\phi_a \exp(\phi_a)}{\exp(\phi_a) - 1} \quad (13)$$

which simulates the effects of suction on any variable being transferred (i.e., mass, momentum and/or energy). In spite of the apparent structural difference between eqs. (12) and (13), they are comparable, exhibiting a close qualitative and quantitative similarity (Herranz et al., 2002).

The natural convection correlation used to estimate the Sherwood number (according to heat-mass transfer analogy) was:

$$Sh = 0.13 \cdot Gr^{1/3} \cdot Sc^{1/3} \quad (14)$$

The Grashof number is dependent on both temperature and composition differences and it should be estimated as:

$$Gr = \frac{g \cdot \rho_{gb} \cdot (\rho_{gi} - \rho_{gb}) \cdot L^3}{\mu^2} \quad (15)$$

## 5. VALIDATION OF THE MODEL

The model presented was validated against the database described above (Anderson et al., 1998). Here below some comparisons are shown to analyse the overall model performance as well as its capability to reproduce specific variable effects. Empirical correlations derived from other databases have also been included to extend this validation (Dehbi et al., 1991; Kataoka et al., 1992):

$$h_{Dehbi} = \frac{L^{0.05} \cdot [(3.7 + 28.7 \cdot P) - (2438 + 458.3 \cdot P) \cdot \log W]}{T_b - T_w} \quad (16)$$

$$h_{Uchida} = 380 \cdot \left( \frac{W}{1-W} \right)^{-0.7} \quad (17)$$

$$h_{Tagami} = 11.4 + 284 \cdot \frac{1-W}{W} \quad (18)$$

$$h_{Kataoka} = 0.43 \cdot \left( \frac{W}{1-W} \right)^{-0.8} \quad (19)$$

### 5.1. Overall performance

A total of 75 tests have been simulated and the results obtained have been plotted versus the experimental measurements (Figure 7).

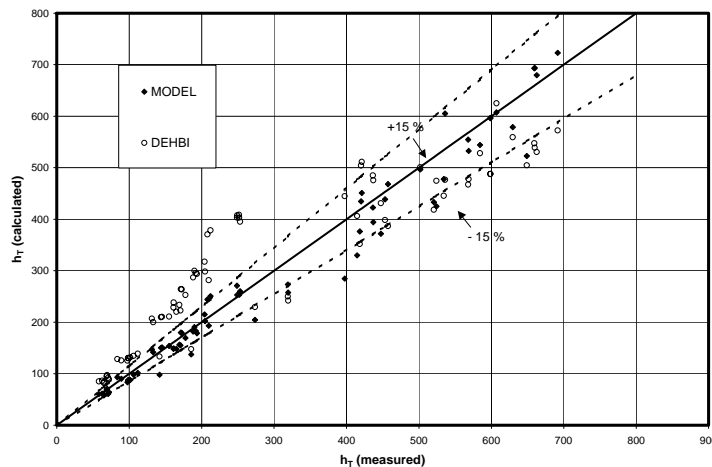


Figure 7. Overall model performance

The lines of  $\pm 1.15\%$  of the measurements have been included to point out the remarkable accuracy of the model. As can be observed, practically all the points are within the band, and less than 15% show greater deviations (most of them underpredictions). The average error is around 12.0%. Dehbi's correlation, however, showed an error around 43%.

### 5.2. Noncondensable concentration

The total heat transfer coefficient has been plotted versus the ratio of air and steam mass fractions (Figure 8). Experimental data recorded by both HFM (*Heat Flux Meters*) and CEB (*Coolant Energy Balance*) have been included along with the model predictions.

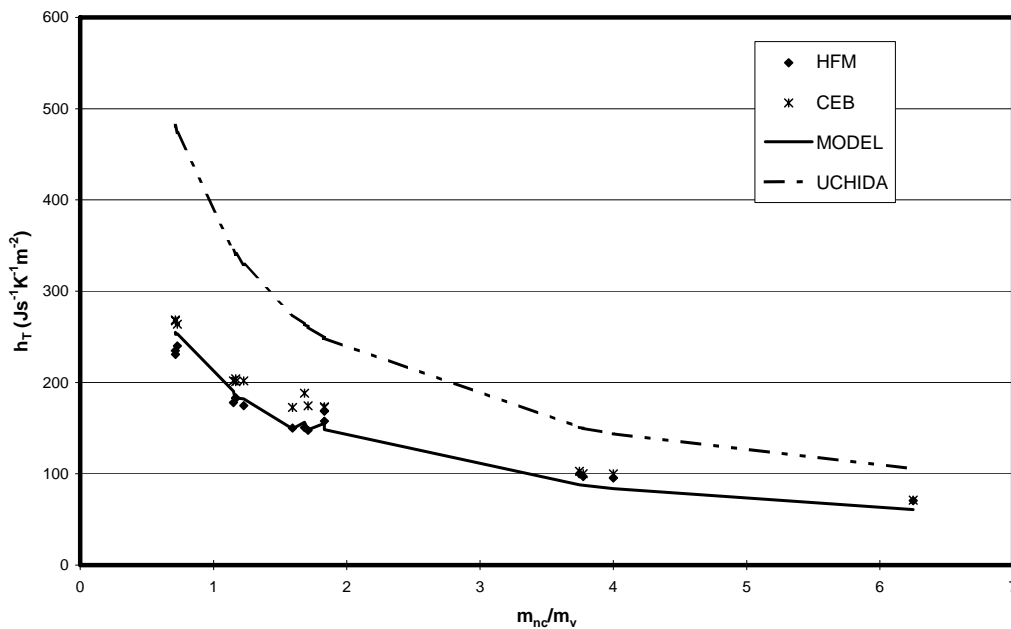


Figure 8. Model response to noncondensable concentration.

The agreement between the estimates and the data is quite good. The model follows the experimental trends remarkably well and shows a power law decay of HTC (*Heat Transfer Coefficient*) with the amount of noncondensable gas. The predictions are located between the different measurement techniques for ratios lower than about two and underestimate the test data for higher ratios. The standard deviations of the model with respect to HFM and CEB are approximately 8.0% and 12.3%, respectively, these numbers being well within the experimental error reported (Anderson, 1998).

Uchida's prediction for these tests have been included in the figure. As can be seen, the similarity between Uchida's and the model's behavior is good. However, a significant quantitative discrepancy can be noted. The experimental procedure used by Uchida allowed a simple correlation of his data (Eq.(17)), but it restricted their reliability to scenarios in which the noncondensable partial pressure ( $P_{nc}$ ) at ambient conditions is 1.0 bar. Peterson (1996) showed that at  $P_{nc} < 1.0$  bar, Uchida correlation tends to overpredict heat transfer coefficients (this was the case for the experiments reported in the figure), whereas at  $P_{nc} > 1.0$  bar the opposite behavior should be expected.

5.3. Noncondensable composition

Figure 9 shows the variation of HTC with the total molar fraction of helium ( $X_{He}$ ) by the model for experiments containing 32% of helium in the noncondensable gas (atmospheric pressure). The quantitative agreement of measurements and estimates is outstanding with respect to both HFM (10.2%) and CEB (8.2%). The decay observed in both measured and calculated HTC's is a consequence of steam depletion and should not be associated with the increase of helium concentration in the gas; namely, no significant effect due to helium presence was noted experimentally and has been theoretically confirmed. The neutral behavior of helium concerning HTC influence has been reported also by other authors (Pernsteiner et al.,1993). Herranz et al. (1998) mechanistically demonstrated that this behavior is a result of the balance between the steam diffusion enhancement and the inhibition of buoyant gas motion caused by the replacement of air molecules by helium ones in the noncondensable gas mixture.

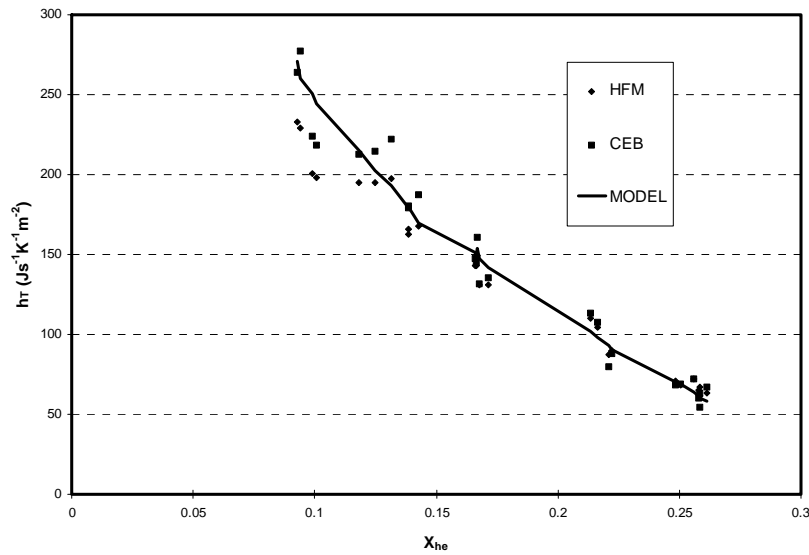


Figure 9. Model response to noncondensable concentration at atmospheric pressure.

In addition to the atmospheric tests, Anderson et al. (1998) performed experiments at higher pressure ( $P = 3\text{bar}$ ). The test conditions and results, together with the model calculations are presented in Table 2. It can be noted that the model results are close to the measurements, the average error 5 being 17.1% (HFM) and 20.1% (CEB). Another set of estimates obtained using Dehbi's correlation for helium (Dehbi et al.,1991) has been also included.

| $T_b$ (C) | $T_w$ (C) | $X_{nc}$ | $X_{He}$ | $h_T$ ( $J s^{-1} m^{-2} K^{-1}$ ) |       |       |       |
|-----------|-----------|----------|----------|------------------------------------|-------|-------|-------|
|           |           | He       |          | HFM                                | CEB   | Model |       |
| 117.7     | 76.9      | 0.0      | 0.0      | 593.7                              | 478.4 | 605   | 503.5 |
| 114.5     | 71.1      | 0.10     | 0.045    | 503.5                              | 410.9 | 468.3 | 386.6 |
| 104.6     | 59.9      | 0.144    | 0.087    | 315.8                              | 323.0 | 257.6 | 241.9 |

|       |      |       |       |       |       |       |       |
|-------|------|-------|-------|-------|-------|-------|-------|
| 105.7 | 61.3 | 0.230 | 0.135 | 335.8 | 302.3 | 273.4 | 249.9 |
| 91.9  | 45.9 | 0.375 | 0.281 | 187.6 | 183.6 | 137.3 | 147.8 |

Table 2. Experimental conditions, test results and theoretical predictions of helium tests at high pressure

### 5.4. Subcooling

In Figure 10 the experimental data along with the model results are presented for atmospheric pressure. The model showed a good qualitative agreement with the data, showing the same trend: HTC diminishes as wall temperature decreases (this negative slope is, however, contrary to the positive one encountered for heat flux). The major deviations of the model are conservative and appear at high subcoolings. The standard deviation of the model is about 13% and 17.5% with respect to HFM and CEB, respectively.

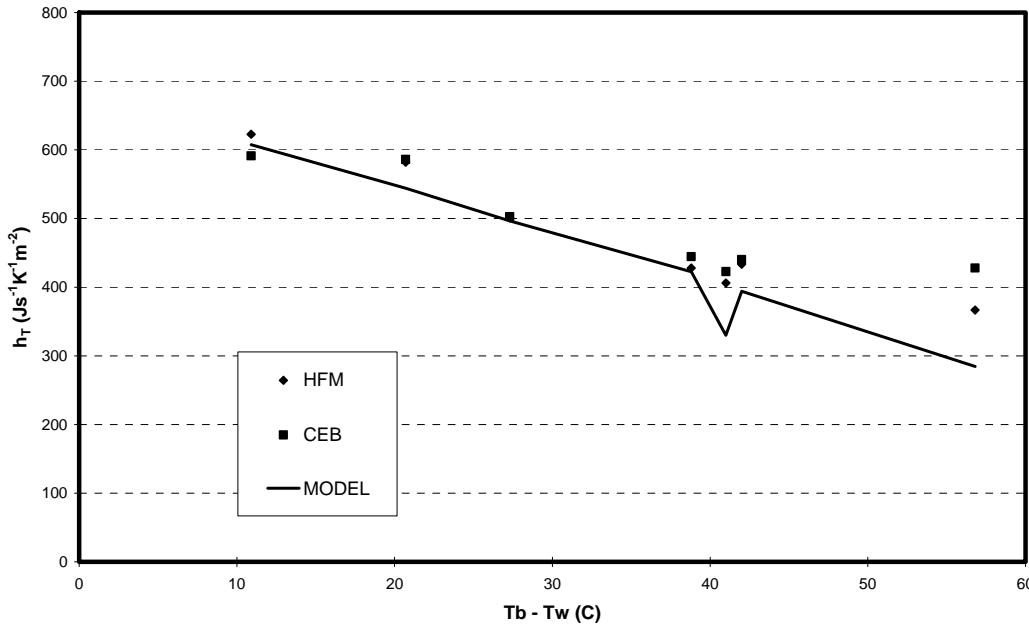


Figure 10. Model sensitivity to subcooling at atmospheric pressure.

Figure 11 presents the variation of HTC with subcooling at 3.0 bar. Along with the data and the model predictions, other correlations have been included. Consistent with the atmospheric pressure, a remarkable agreement between data and calculations have been found both qualitatively and quantitatively. The standard deviations with respect to HFM and CEB are 9.5% and 12.2%, respectively. Dehbi's correlation results behaves similarly to the model's, but their errors were slightly higher. Unlike Dehbi's, the rest of correlations do not show any sensitivity to the subcooling when  $\Delta T_{bw}$  variation is due to a change in  $T_w$  instead in  $T_b$  (the light variations observed are precisely due to  $T_b$  fluctuations). This behavior is not unexpected since the experimental procedure used in Uchida's, Tagami's and Kataoka's tests kept  $T_w$  constant. The low values of the HTC's estimated by these correlations could be attributed to lower gas bulk velocities in their experimental facilities as compared to the scenario velocities expected in a representative scenario.

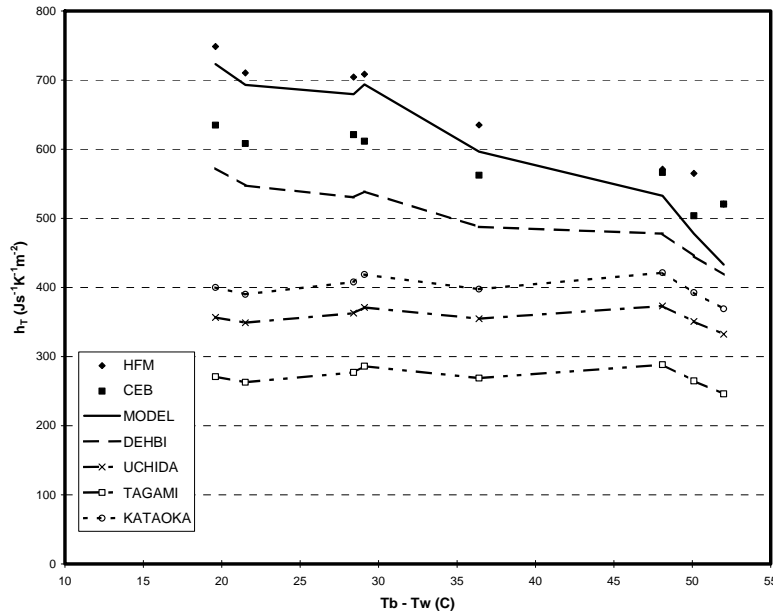


Figure 11. Model sensitivity to subcooling at high pressure (3 bar).

### 5.5. Pressure

Figure 7 shows the experimental variation of the HTC's as a function of pressures along with model's predictions. The model showed a trend similar to data's and a good quantitative agreement, with an average error of approximately 20% with respect to both HFM and CEB measurements.

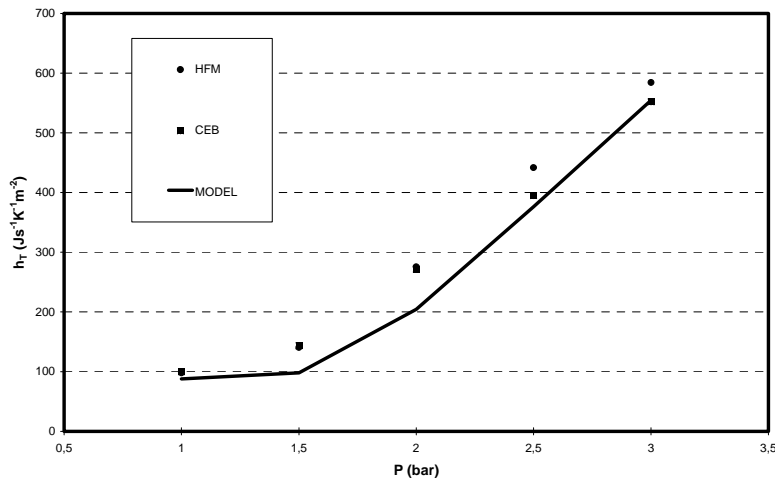


Figure 12. Model sensitivity to pressure.

In order to extend the model validation to other databases, Dehbi's data (Dehbi,1991) were also considered. Dehbi et al. carried out three sets of experiments in the presence of air at 1.5, 3.0 and 4.5 bar. The air mass fraction varied between 25% and 90% while the wall temperature subcooling varied from 15 to 50 °C. In Table 3 the conditions, results and error analysis for nine of Dehbi's tests are presented. Each experimental series consists of three tests with different noncondensable mass fractions. Some boundary conditions are approximated as average values, since variables such as  $T_w$  y  $T_b$  showed noticeable variations along the length of the test section.

|                          | Series A                               |       |       | Series B |       |       | Series O |       |       |
|--------------------------|--|-------|-------|----------|-------|-------|----------|-------|-------|
|                          | <i>Experimental Conditions</i>         |       |       |          |       |       |          |       |       |
|                          | A38                                    | A30   | A25   | B39      | B33   | B28   | 025      | 016   | 09    |
| <i>T<sub>b</sub> (O)</i> | 101                                    | 94    | 79    | 125      | 113   | 85    | 137      | 127   | 95    |
| <i>T<sub>w</sub> (O)</i> | 72                                     | 65    | 60    | 90       | 88    | 62    | 100      | 82    | 60    |
| P (bar)                  | 1.5                                    | 1.5   | 1.5   | 3.0      | 3.0   | 3.0   | 4.5      | 4.5   | 4.5   |
| W                        | 0.33                                   | 0.56  | 0.80  | 0.34     | 0.59  | 0.85  | 0.35     | 0.58  | 0.88  |
|                          | <i>Heat Transfer Coefficients (SI)</i> |       |       |          |       |       |          |       |       |
| Test                     | 788.4                                  | 461.2 | 189.7 | 981.8    | 502.1 | 141.3 | 1171.5   | 606.2 | 178.5 |
| Model                    | 647.7                                  | 360.9 | 151.9 | 1176     | 533.5 | 122.5 | 1246     | 577.1 | 136.6 |
| Dehbi                    | 577.9                                  | 365.1 | 189.1 | 862.8    | 457.7 | 154.8 | 906.7    | 505.4 | 172.8 |
| U chida                  | 491.9                                  | 307.0 | 152.0 | 642.6    | 294.2 | 99.9  | 559.7    | 311.8 | 97.7  |
| Tagami                   | 422.1                                  | 220.8 | 88.1  | 612.9    | 208.4 | 53.5  | 505.3    | 225.4 | 52.2  |
| Kataoka                  | 577.6                                  | 337.0 | 150.9 | 783.8    | 320.9 | 93.4  | 669.4    | 342.9 | 91.0  |
|                          | <i>Error Analysis (%)</i>              |       |       |          |       |       |          |       |       |
| Model                    | 17.8                                   | 21.7  | 19.9  | 19.8     | 6.2   | 13.3  | 6.3      | 4.8   | 23.5  |
| Dehbi                    | 26.7                                   | 20.8  | 0.3   | 12.1     | 8.8   | 9.5   | 22.6     | 16.6  | 3.1   |
| U chida                  | 37.6                                   | 33.4  | 19.9  | 34.5     | 41.4  | 29.3  | 52.2     | 48.6  | 45.3  |
| Tagami                   | 46.5                                   | 52.1  | 53.5  | 37.6     | 58.5  | 62.1  | 56.9     | 62.8  | 70.7  |
| Kataoka                  | 26.7                                   | 26.9  | 20.4  | 20.2     | 36.1  | 33.9  | 42.8     | 43.4  | 48.9  |

Table 3. Comparison of model to other correlations under Dehbi's tests conditions

The results in the table show a good consistency between the model's predictions and the experimental results. The experimental variations of HTC's with pressure and noncondensable content have been reproduced with the model. The average error has been found to be 17.3%. This error is very similar to the one resulting from model validation against Anderson's data above and, furthermore, it is very close to the standard deviation shown by Dehbi's correlation if the boundary conditions shown in the table are used (16.8%). Uchida's, Tagami's and Kataoka's correlations show average errors higher than 35% in all the cases.

## 6. FINAL REMARKS

This paper shows that experimental investigations related to Westinghouse's AP600 nuclear reactor have been performed and the in-depth study has generated a valuable data base to validate models and has pointed out several interesting phenomena that should be considered when modeling condensation under this range of conditions:

- The use of a more sophisticated equations than simple correlations based on the  $W_{nc}/W_v$  ratio is required to achieve accurate estimates of heat transfer under the natural convection prevailing in future AP600 containments.
- The increase in pressure causes an increase the HTC and it is usually associated to concentration changes that drive to even more significant than the pressure enhancement itself.
- Stratification of light noncondensable gases in the containment could affect dramatically heat transfer by condensation as their concentration exceeds approximately 40% molar with respect to the air. Under these conditions stratification prohibits condensation and can result in as much as a 50% reduction in the heat transfer.

In addition, the paper presents a model based on the diffusion layer theory and the heat mass transfer analogy. By comparing its predictions and data its capability to simulate accurately the foreseen conditions in the AP600 containment has been demonstrated. Likewise, the model has been shown to be a useful tool to interpret condensation phenomena, providing theoretical insights into the influence of variables such as pressure or light gases presence in the noncondensable mixture. Finally, cross comparisons with credited correlations in containment nuclear safety and others more recently developed have highlighted shortcomings inherent to such correlations, underlining the advantages of using more mechanistic approaches to simulate phenomena involved in postulated accidents.

## 7. REFERENCES

- J.K. Aggarwal, M. A. Hollingsworth, Heat Transfer for Turbulent Flow with Suction in a Porous Tube, *Int. J. Heat Mass Transfer* 16 (1973) 591-609.
- M.H. Anderson, L.E. Herranz, M.L. Corradini, Experimental Analysis of Heat Transfer within the AP600 containment under Postulated Accident Conditions, *Nuclear Engineering and Design*, Vol. 185, ns. 2-3, 153-172, 1998.
- R. B. Bird, W.E. Stewart, E. D. Lightfoot, *Transport Phenomena*, Chapter 21, John Wiley Interscience Editions, 1960.
- R.S. Bunker, V.P. Carey, Modelling of Turbulent condensation Heat transfer in the Boiling Water Reactor Primary Containment, *Nucl. Engrg. Des.* 91 (1986) 297-304.
- J.G. Collier, J.R. Thome, *Convective Boiling and Condensation*, Chapter 10, 3rd ed., Oxford University Press, Oxford (1994).
- M.L. Corradini, Turbulent Condensation on a Cold Wall in the Presence of a Noncondensable Gas, *Nucl. Techn.* 64 (1984) 186-195.
- A.A. Dehbi, M.W. Golay, M.S. Kazimi, 'Condensation Experiments in Steam-Air and Steam-Air-Helium Mixtures under Turbulent Natural Convection, National Conference of Heat Transfer (1991), AIChE Sym-

posium Series, 19-28.

S.M. Ghiaasiaan, B.K. Kamboj, S.I. Abdel-Khalik, Two-Fluid Modeling of the Condensation in the Presence of Noncondensable in Two-Phase Flows, Nucl. Sci. Engrg. 119 (1995) 1-17.

J. Green, K. Almenas, An Overview of the Primary Parameters and Methods for Determining Condensation Heat Transfer to Containment Structures, Nuclear Safety, Vol. 37, No. 1 (1996) 26-47.

J.F. Herr, J.R. Kadambi, Effect of Non-Condensable Gases on Condensation Heat Transfer, Proceedings of the Fluid Engineering Conference (1993) 77-86.

Herranz, L.E. 1996. Desarrollo y validación de modelos avanzados de transmisión de calor en los condensadores de refrigeración pasiva de la contención SBWR. Doctoral Thesis. Polytechnic University of Madrid, Madrid, Spain.

L.E. Herranz, J. L. Munoz-Cobo, G. Verdu, Heat Transfer Modeling in the Vertical Tubes of the Passive Containment Cooling System of the Simplified Boiling Water Reactor, Accepted for publication in the Nucl. Engrg. Des. (1997).

L.E. Herranz, M.H. Anderson, M.L. Corradini, "A diffusion layer model for steam condensation within the AP600 containment", Nuclear Engineering and Design, Vol. 183, ns. 1-2, 133-150, July 1998.

L.E. Herranz, A. Campo, "On the adequacy of heat-mass transfer analogy to simulate containment atmospheric cooling in the new generation of advanced nuclear reactors: experimental confirmation", Nuclear Technology 139, 221-232, 2002.

I. K. Huhtiniemi, M. L. Corradini, Condensation in the presence of nonecondensable gases, Nuclear Engrg. Des. 141 (1993)

Y. Kataoka, T. Fukui, S. Hatamiya, T. Nakao, M. Naitoh, I. Sumida, Experiments on Convection Heat Transfer Along a Vertical Flat between Pools with Different Temperatures, Nucl. Techn. 99 (1992) 386-396.

M.D. Kennedy, F.E. Peters, M.D. Carelli, A.T. Pieczynski, Advanced PWR Passive Containment Cooling system Testing, Proceedings of the ARS'94 International Topical Meeting on Advanced Reactor Safety, April 1994, Vol. 1, 249-256.

M.H. Kim, M.L. Corradini, Modeling of Condensation Heat Transfer in a Reactor Containment, Nucl. Engrg. Des. 118 (1990) 193-212.

S.Z. Kuhn, V.E. Shrock, P.F. Peterson, An Investigation of Condensation from Steam-Gas Mixtures Flowing Downward Inside a Vertical Tube, Proceedings of the Seventh International Topical Meeting on Reactor Thermalhydraulics, NURETH-7, Sept. 1995, 312-335.

Mickley, H.S. 1954. Heat, mass and momentum transfer for flow over a flat plate with blowing or suction. NACA-TN-3208.

D.G. Ogg, Vertical Downflow Condensation Heat Transfer in Gas-Steam Mixtures, M.S. Thesis, Department of Nuclear Engineering, University of California, Berkeley 1991.

A. Pernsteiner, I.K. Huhtiniemi, M.L. Corradini, Condensation in the Presence of Noncondensable Gases: Effect of Helium, Proceeding of the NURETH-6 Conference (1993).

**L.E. Herranz et al.**

P.F. Peterson, V.E. Shrock, T. Kageyama, Diffusion Layer Theory for Turbulent Vapour Condensation with Noncondensable Gases, *Journal of Heat Transfer* 115 (1993) 998-1003.

C. Sawyer, Thermal/Hydraulic Challenges for the SBWR, Proceedings of the Fifth International Topical Meeting on Reactor Thermalhydraulics, NURETH-5 "Towards the Next Generation of Nuclear Reactors", Sept. 1992, Vol. 1, 21-24.

M. Siddique, M.W. Golay, M.S. Kazimi, Local Heat Transfer Coefficients for Forced Convection Condensation of Steam in a Vertical Tube in the Presence of a Noncondensable Gas, *Nucl. Techn.* 102 (June 1993), 386-402.

E.M. Sparrow, S.H. Lin, Condensation Heat Transfer in the Presence of a Noncondensable Gas, *Journal of Heat Transfer* (August, 1964) 430-436.

D. R. Spencer, J. Woodcock, R. F. Wright J. A. Gresham, "Westinghouse - Gothic Comparison with Passive Containment Cooling System Tests Scaling Evaluation and Analysis", ASME/JSME Nuclear Engineering Conference, 1, AS ME 1993.

T. Tagami, Interim Report on Safety Assessments and Facilities Establishment Project for June 1965, No. 1, Japanese Atomic Energy Research Agency, unpublished work (1965).

J.J. Taylor, Safety Characteristics of Future LWR's, Proceedings of the International ANS/ENS Topical Meeting on Thermal Reactor Safety, Section XIV, San Diego, CA (1986).

H. Uchida, A. Oyama, Y. Togo, Evaluation of Post-Incident Cooling Systems of Light-Water Power Reactors, Proceedings of International Conference on Peaceful Uses of Atomic Energy, 13 (1965) 93-102.

K.M. Vierow, V.E. Schrock, Condensation in a Natural Circulation Loop with a Noncondensable Gas Present, Proceedings of the International Conference on Multiphase Flow, Tsukuba, Japan 1991, 183-186.

Class 2 WCAP, AP600 1/8th Large Scale Passive Containment Cooling System Heat Transfer Test Baseline Data Report, WCAP-13566 (1992).

V.M. Yeroshenko, A. V. Yershov, L.I. Zaichik, Heat Transfer for Turbulent Flow in a Circular Tube with Suction or Injection, *Int. J. Heat Mass Transfer* 27, 8 (1984) 1197-1203.

R.Y. Yuann, V.E. Schrock and X.M. Chen, Numerical Modeling of Condensation from Vapor-Gas Mixtures for the Forced Downflow inside a tube, Proceedings of the Seventh International Topical Meeting on Reactor Thermalhydraulics, NURETH-7, Sept. 1995,